N95- 20515

AMORPHOUS SILICON THIN FILMS: THE ULTIMATE LIGHTWEIGHT SPACE SOLAR CELL

G.J. Vendura, Jr., M.A. Kruer, H.H. Schurig, M.A. Bianchi, and J.A. Roth
TRW Space and Technology
Redondo Beach, California

ABSTRACT

Progress is reported with respect to the development of thin film amorphous (α-Si) terrestrial solar cells for space applications. Such devices promise to result in very lightweight, low cost, flexible arrays with superior end of life (EOL) performance. Each α-Si cell consists of a tandem arrangement of three very thin p-i-n junctions vapor deposited between film electrodes. The thickness of this entire stack is approximately 2.0μm, resulting in a device of negligible weight, but one that must be mechanically supported for handling and fabrication into arrays. The stack is therefore presently deposited onto a large area (12 by 13 in.), rigid, glass superstrate, 40 mil thick, and preliminary space qualification testing of modules so configured is underway. At the same time, a more advanced version is under development in which the thin film stack is transferred from the glass onto a thin (2.0 mil) polymer substrate to create large arrays that are truly flexible and significantly lighter than either the glassed α-Si version or present conventional crystalline technologies. In this paper the key processes for such effective transfer are described. In addition, both glassed (rigid) and unglassed (flexible) α-Si cells are studied when integrated with various advanced structures to form lightweight systems. EOL predictions are generated for the case of a 1000 W array in a standard, 10 year geosynchronous (GEO) orbit. Specific powers (W/kg), power densities (W/m^2) and total array costs ($/$ft^2$) are compared.

INTRODUCTION

During the next ten years, spacecraft power requirements will grow significantly over the presently typical 1 to 4 kW EOL systems. Also, more interest will be focused upon smaller and lighter systems in the 0.1 to 1.5 kW range. Finally, the proliferation of small, less expensive launch vehicles will require low-mass, low cost, power sources. Current crystalline silicon technology using 8 mil thick devices is too heavy, costly and large to support higher power levels on satellites thrust into space by existing and planned vehicles. Thin, 13.5% efficient, silicon cells and even higher efficiency gallium arsenide and indium phosphide cells reduce weight and area but increase cost. New generation lightweight photovoltaic devices are required to meet this challenge (ref. 1). These new devices, by nature, are expected to be both enhancing and enabling: enhancing by offering advantages in power, weight and cost compared to traditional crystalline solar cells in existing satellite designs for conventional orbits; enabling by extending array and mission capability beyond the present limitations of such space systems.

For this reason, thin film solar cells are presently generating intense interest within the space community. Those technologies that have already enjoyed significant development for terrestrial applications are especially attractive. Both α-Si and copper indium diselenide (CIS) fall into this category, but of the two, α-Si is by far the more advanced (ref. 2-3). Very large area α-Si cells and integrated modules are already routinely manufactured for terrestrial applications with AMO efficiencies of 8 to 10%. Although this is considerably less than standard 13.5 and 18.5% Si and GaAs/Ge figures, the material's greater radiation resistance, ultra light weight, low cost, flexibility and the ability to be incorporated into existing, well-developed, lightweight, satellite array structures makes α-Si not only a viable but also a potentially superior alternative. Significantly, the cells can be interconnected in various series and parallel configurations by means of standard semiconductor monolithic integration techniques resulting in superior packing densities and the reduction in the yield and cost disadvantages associated with numerous discrete parts and corresponding handling operations.

α-Si SPACE SOLAR CELL APPROACH

The α-Si solar cell chosen for such space development, shown in Figure 1, is routinely fabricated by Solarex Thin Films and allows the maximum leverage of existing terrestrial technology (ref. 4). The active material consists of a stack of three individual α-Si p-i-n cells sandwiched between thin electrodes. The upper electrode of SnO_2 is transparent to incident light, while the back electrode of silver is opaque. The three α-Si cells are not compositionally identical. Instead, uppermost and lowermost devices are carbon and germanium alloys respectively to allow for increased collection efficiency by utilizing a broader segment of the solar spectrum. The entire stack has a total cross section of only 2.0μm. However, the commercial product is deposited upon a 40 mil superstrate of either soda lime or borosilicate glass as a means of mechanical support during fabrication and handling. Although both single junction and double junction variations of this device are manufactured on superstrates as large as 4 square feet, the baseline space product considered in this study is limited to 12 by 13 in.

The effort to develop this terrestrial commercial product into a device suitable for space can be divided into two major phases:

I. Development and qualification testing of these glassed 12 by 13 in. terrestrial cells to create a usable, rigid space product. Although the superstrate contributes significantly to overall weight, results of early cost and power trades indicate advantages for certain missions.

II. Development of materials and additional processes for transferring 3 by 3 in. areas from the glass superstrate onto a thin, polymer substrate to demonstrate a flexible space product. Earlier stages will focus primarily on mechanical issues, while later stages will address both mechanical and electrical stability. A later phase will concentrate on the scaling up of these processes to transfer 12 by 13 in. and larger areas.

The most important aspects of the Phase I effort center on radiation and temperature effects and long term stability. Studies by Woodyard and co-workers indicate that radiation damage, in large part, may be reversed by annealing (ref. 5). Also, attention must be focused on the degradation of α-Si output due to photons (the Staebler Wronski effect) and its reduction (ref. 6-7). Significant adjustments in the manufacturing sequence have already been made by Solarex and will continue to be considered to minimize this effect.

ADVANCED PROCESSES

Phase II, addressed simultaneously with Phase I to save time, focuses on the materials and process development of two key additional processes required for transfer: release and liftoff. These processes are illustrated in Figure 2 on the right, while the standard commercial sequence is shown on the left. The release process consists of sputter deposition of carefully controlled thin film layers directly onto the glass superstrate to partially isolate it mechanically and chemically from the commercial device that is deposited subsequently. This limits the adhesive strength which, in turn, facilitates eventual separation. The liftoff process, on the other hand, involves the attachment of polymer and other films to the back surface of the commercial stack by means of a thermo-compression technique. The number and orientation of these backing layers are carefully balanced to create the right relative mismatch in the various coefficients of thermal expansion. As a result of differential contraction upon cooling, separation at the release interface is accomplished and the solar cell is thereby transferred from the rigid, glass superstrate onto the flexible, laminated substrate.

The release process is dependent upon very specialized, large-scale sputtering equipment. Either of two custom built sputtering machines can be used, depending upon solar cell size and quantity. Although cells of 12 by 13 in. are presently earmarked for the baseline process, individual device areas are expected to eventually increase to 4 and 8 ft^2. It is advantageous to load large batches of such cells into a single machine for economy.

The chamber of the first unit is 6.0 by 6.0 by 6.0 ft. and can be evacuated to the low 10^{-7} torr range by a 16 in. cryopump. The machine can operate in RF or DC modes and is equipped with three 5.0 by 20.0 in. targets, capable of co-deposition onto three 20.0 by 20.0 in. substrates rotating via a planetary. Operation is computer driven and monitored to permit unattended deposition of multiple layers. Control devices include an in situ particle counter, a quartz crystal thickness monitor, a residual gas analyzer and an optical monitor to track reflective interference to a quarter of a wavelength.

The second sputtering machine consists of a chamber with a floor area 20 by 12 ft. and a ceiling 15 ft. high. Overnight evacuation to the low 10^{-7} torr is achieved by three 16 in. and one 48 in. cryopumps coupled to a Woods Root blower. The machine is fitted with three 5 by 40 in. planar cathodes that move in a raster pattern from 0.5 to 36 in. away from a substrate as large as 18 ft. long and 12 ft. high. Co-deposition is possible via two of the three targets. By means of another cathode assembly, 10 in. round, non-planar shapes can be coated. This machine can also operate in either RF or DC modes, is similarly computer controlled and monitored, and is fitted with a residual gas analyzer, a quartz crystal monitor and a particle counter.

An earlier version of the overall release process involved the deposition in the smaller machine of three separate layers, shown in Figure 3a. After cleaning, the glass superstrate was loaded into the chamber which was then evacuated to 10^{-6} torr. A 400Å layer of binder material was deposited. The purpose of this film was to promote adhesion between the glass surface and subsequent materials: a release layer of approximately 800Å followed by a 1.5 μm cap of SiO_2. The purpose of the release layer is to provide a release interface (R.I.) - a plane of significantly weaker chemical and mechanical adhesion compared to all other interfaces - so that separation can eventually be achieved at this surface.

After deposition of these three layers, the treated glass was shipped to Solarex, where the α-Si solar cell components (Figure 1) were added. The device was then returned. Initial liftoff experiments, intended to separate the cell at the R.I., produced mixed results. In some cases the solar cell did not release at all; in others, release was uneven. EDAX and SEM investigations of suspect areas of the surface seemed to indicate atomic diffusion of the superstrate across the release layer resulting in pinning - localized areas of high adhesion - at the R.I. Since the commercial fabrication sequence involves SnO_2 and contact annealing processes that approach the softening point of glass, a high temperature mechanism was suspected.

To eliminate this pinning without affecting the solar cell manufacturing sequence, the release process was modified to include a 400Å diffusion barrier as shown in Figure 3b. An additional 800Å layer varying in composition from barrier to release layer materials was also necessary to ensure the R.I. remained the weakest link in the chain of interfaces in order to prevent separation at the barrier-release layer surface instead.

Again the treated glass was shipped to Solarex and returned with solar cells attached. Experiments demonstrated significantly improved results, although the process continues to be developed further.

The liftoff process involves the attachment of five plies of flexible material to the back surface of the cell in three stages. As shown in Figure 4, three layers of 1.0 mil polymer are interspersed with two 1.0 mil layers of fiberglass cloth. In the first stage, all but one polymer layer are aligned, placed in vacuum, degassed and subjected to a two step cure process. The second stage consists of surface preparation of the Ag contact on the back of the solar cell, followed by mechanical placement of the remaining polymer film. In the third stage, all parts are joined into a single unit by an additional vacuum, degas, and cure sequence. Under ideal conditions, upon cooling, the solar cell releases spontaneously and cleanly at the R.I. due to a differential in the coefficients of thermal expansion (CTE).

The CTEs are balanced by careful selection of layer composition, thicknesses and orientations. For example, the two fiberglass cloth plies are aligned in different directions, one at 0,90 degrees and the other at ±45 degrees, as implied by the dissimilar slash patterns in Figure 4. Another key concern is the complete elimination of air bubbles during processing. Air bubbles result in voids - points of no adhesion between the flexible substrate and the solar cell. Thus, upon release of the bulk of the α-Si, areas under

the voids can remain behind, creating pinholes in the surface of the cell which in turn may result in shorting and power degradation.

Figure 4 is representative of one of several variations of the liftoff process still under development. Other variations use different quantities of layers or plies of different thickness. The objective, however, is to eliminate layers or to use thinner plies so that the total flexible substrate is approximately 2.0 mil.

LIGHTWEIGHT STRUCTURES

α-Si cells, both glassed (Phase I) and flexible (Phase II), are suitable for incorporation into conventional and low mass arrays. For the purposes of comparison, a 1000 W array was considered. In the first case a state-of-the-art 0.5 in. thick Al honeycomb with 5.0 mil graphite face sheets and a single layer of 2.0 mil Kapton to insulate the solar cells is assumed. In addition, two existing, well-developed lightweight structures were studied. The first is an adaptation of the Advanced Photovoltaic Solar Array (APSA) (ref. 8). The original APSA consisted of a 5.4 kW, 15.25 by 2.81 m, mast-deployed, 42 panel, prototype wing as shown in Figure 5 (ref. 9). This unit was populated by 2.2 mil thick crystalline silicon solar cells, 2.0 by 4.0 in. area, with 2.0 mil cover glasses. The efficiency of these cells was 13.5%. A key lightweight feature is the employment of a 2.0 mil carbon loaded Kapton substrate, accordion folded for stowage during launch. Despite this lightweight blanket, however, major contributions to mass resulted from the deployment mast, the frame and the stowage container. Since this study concerns an array less than 25% of the original APSA area, wherever possible, features such as this container size were scaled down accordingly.

Another advanced lightweight structure involved using a TRW developed and tested framed membrane technology. Main features of such a system, highlighted in Figure 6, include a rigid membrane solar cell support consisting of a very thin laminate with a foam core and high modulus, graphite fiber reinforced plastic (GFRP) face sheets. Kapton is used to insulate the solar cells from the membrane surface. The frame tubes are transfer molded from a mixture of high modulus and high strength GFRP materials. To create a panel structure subassembly, the various GFRP components are joined together through a precision bonding process without the need for mechanical fasteners. Such a panel design is adaptable for use with cells of various types, sizes and thicknesses and can be readily scaled up or down as required. An advanced version of the system involves lighter frame and substrate elements. Indeed, an adaptation of the system, using a different rigid laminate and no frame whatsoever, was incorporated in the Earth Observing System (EOS) program.

The ultimate lightweight array, the Ultra Light Film Array (ULFA), is presently limited to satellites $\leq$1000W. It includes a 2.0 mil flexible Kapton blanket, but not the relatively heavy components of either the APSA or framed membrane designs. In this case, the blanket is deployed and supported by lightweight strain energy hinges. Although development of such a structure is not as mature as APSA and membrane technologies, it is nonetheless included in this study for comparison purposes.

RESULTS

Results are in the form of EOL performance predictions of satellite systems incorporating various α-Si and conventional crystalline solar cells populating the four structures described. In all cases, a standard, 10 year GEO mission is assumed for the nominal 1000 W array. Weight of stowage and deployment hardware is included. In the case of α-Si arrays, cell interspacing was set at 120 mil, while for crystalline devices it was 30 mils. Also, whenever possible, proven cell and system design factors were used. For example, empirical loss factors were applied to account not only for temperature and radiation degradation, but also for more obscure losses such as Staebler Wronski (SW), packing, wiring, installation, cycling, cover glass darkening, etc. All comparisons are thus at a system level of performance as opposed to often quoted device or cell level performance. It is noted, however, that all systems are not universally applicable to all cells, and in certain specific cases some overdesign and underdesign is inevitable. Therefore, the accuracy of results is estimated to be $\pm$10%.

Data are summarized in Table 1 for 13 different systems. Rows 1 through 4 present data for unannealed α-Si having 4 different cover glass thicknesses: 40 mils, 8 mils 2μm and 1 mil. Systems 5 through 7 outline crystalline Si, while 8 and 9 highlight crystalline GaAs/Ge. Rows 10 through 13 examine the same α-Si systems as 1 through 4, but this time the systems are designed for self annealing, resulting in considerable radiation and Staebler Wronski loss recovery. Details such as cell type, size, device and cover thicknesses and BOL efficiency, η, are presented in the leftmost columns. For α-Si, BOL η was assumed to be a conservative 10.0% at AMO and 28°C. Crystalline η, on the other hand, varied from 12.2 to 18.2% as tabulated. Staebler Wronski degradation is assumed at 15% for unannealed α-Si and 5% for the same cells when annealed. In the table, honeycomb, membrane, APSA and ULFA data then follow in terms of three key parameters: specific power (W/kg), power density (W/m^2) and areal density (lbs/ft^2).

In generating these data for the systems involving α-Si, radiation degradation behavior in response to orbital environment was calculated from a model using the standard approach of equating ionization and displacement damage with P/Po power reduction. This technique uses existing data for P/Po from 1MeV proton fluences and extends it to other proton energies. P/Po is defined as a function of 1MeV protons similar to crystalline technology, using 1MeV electrons as the conversion parameter (ref. 10).

The α-Si comparison is presented graphically in Figure 7 in which the structural density (the sum of the system's areal density and the weight of peripheral hardware -hinges, booms, deployment hardware, etc.- spread over array area) is plotted as a function of specific power. As shown, even cells with 40 mil covers generate respectable powers when compared with the ~15 W/kg figure for a crystalline silicon system (not shown) using less than the state-of-the art honeycomb presented in this study. As expected, α-Si with 8 mil covers performs considerably better, especially in the case of APSA in which best results are 77.7 and 83.2 W/kg for unannealed and annealed cells respectively. Note that because of weight, only 2 μm and 1 mil α-Si cells are appropriate for application to the ULFA structure. Here, results as high as 340.9 W/kg are indicated for the annealed 2 μm cover system. Of note is the fact that 1 mil of cover glass and/or annealing makes a considerable difference over an unannealed 2 μm α-Si array incorporated in any structure in the GEO environment.

In Figure 8, less-than-optimal 8 mil covered α-Si is compared to the best of the crystalline Si and crystalline GaAs/Ge systems. The crystalline Si cell used was a 2.5 x 5.0 cm, 2.7 mil thick device with both a back surface field and reflector (BSFR) and a 2.0 mil cover. The GaAs/Ge device was 4.0 x 4.4 cm, 5.5 mils thick, with a 3.0 mil cover. The curves demonstrate that both unannealed and annealed α-Si is superior at structural densities approaching APSA. At higher structural densities, however, α-Si and crystalline Si are comparable, while GaAs/Ge is superior.

In Figure 9, the same crystalline systems are compared with those for the α-Si cell covered with 1 mil of glass. Here the ULFA structure is inappropriate for all but the α-Si case. Best results are 266.5 and 288.3 W/kg for unannealed and annealed devices respectively.

Specific power alone, of course, is not the only major point of comparison. Depending on mission and program constraints, power density, and areal density can also be key considerations. Table 1 also offers these data for the 13 systems under study.

Another essential factor is cost. System cost, typically in $/W, involves the sum of three separate figures: cell materials, structural materials and recurring fabrication labor. Only the first of these is presented in Table 1. The prices of the crystalline cells are well-established, while, admittedly, α-Si figures are rough estimates based upon current commercial terrestrial production prices. Depending on cover glass, these figures may be off by a factor as high as 5. Nevertheless, savings associated with α-Si compared to crystalline systems, depending on choice, readily approach an order of magnitude.

SUMMARY

An approach is described for developing very lightweight α-Si solar cells for space by leveraging progress of terrestrial devices. Glass and flexible versions are being addressed simultaneously. Critical release and liftoff processes for transferring such cells from a rigid 40 mil superstrate onto a flexible 2.0 mil substrate are presented. EOL performance predictions are generated based upon a 10 year GEO mission of a 1000W array incorporating different α-Si and crystalline cell configurations with four distinct structures. Results demonstrate that specific powers of 266.5 and 288.3 W/kg are achieved when α-Si cells with 1 mil covers, unannealed and annealed respectively, are combined with the ULFA structure. The specific power increases further, to 340.9 W/kg for annealed devices with a 2 μm cover. These figures are two to five times better than the performance of conventional crystalline solar cells in similar systems for an identical mission.

REFERENCES

1) Vendura, Jr., G.J.; Malone, P.; and Crawford, L.: A Novel Lightweight Solar Array: Comparison with Conventional Systems. IEEE 23rd Photovoltaic Specialists Conference, Louisville, KY, May 1993, pp. 1381 - 1385.

2) Arya, R.R.; Yang, L.; Bennett, M.; Newton, J.; Li, Y.M.; Fieselmann, B.; Chen, L.F.; Rajan, K.; Wood, G.; Poplawski, C.; and Wilczynski, A.: Status, Progress and Challenges in High Performance Stable Amorphous Silicon Array Based Triple Junction Modules. IEEE 23rd Photovoltaic Specialists Conference, Louisville, KY, May 1993, pp. 790 - 794.

3) Basol, B.M.; Kapur, V.K.; Halani, A.; Minnick, A.; and Leidholm, C.: Modules and Flexible Cells of $CuInSe_2$. IEEE 23rd Photovoltaic Specialists Conference, Louisville, KY, May 1993, pp. 426 - 430

4) Carlson, D.E.: Market, Manufacturing and Technical Progress in Amorphous Silicon Photovoltaics in the U.S. IEEE 22nd Photovoltaic Specialists Conference, Las Vegas, NV, Oct. 1991, pp. 1207 - 1212

5) Woodyard, J.R.; Landis, G.A.: Radiation Resistance of Thin-Film Solar Cells for Space Photovoltaic Power Solar Cells, 31, 1991, pp. 297 - 329

6) Staebler, D.L.; and Wronski, C.R.: Appl. Phys. Lett. (1977) pp. 292

7) Yamagishi, H.; Asaoka, K.; Nevin, W.A.; Yamaguchi, M. and Tawada, Y.: Light Induced Changes of Amorphous Silicon Solar Cells by Long Term Light Exposure. IEEE 22nd Photovoltaic Specialists Conference, Las Vegas, NV, Oct. 1991, pp. 1342 - 1346

8) Kurland, R.M.; and Stella, P.M.: Demonstration of the Advanced Photovoltaic Solar Array. European Space Power Conference, Florence, Italy, Sept. 1991, pp. 675 - 680

9) Stella, P.M.; and Kurland, R.M.: Operational Considerations of the Advanced Photovoltaic Solar Array. 27th Intersociety Energy Conversion Engineering Conference, San Diego, CA, 1992, pp. 6.29 - 6.34,

10) Tada, H.Y.; Carter, Jr., J.R.; Anspaugh, B.E.; and Downing, R.E.: Solar Cell Radiation Handbook, Third Edition, National Aeronautics and Space Administration, Jet Propulsion Laboratory, Nov. 1982.

TABLE 1: PERFORMANCE COMPARISON: CELLS, STRUCTURES & SYSTEMS

	EOL, 10 Year, GEO								Rigid Honeycomb 0.433 lb/ft²**			Framed Membrane 0.300 lb/ft²**			APSA 0.133 lb/ft²**			ULFA 0.032 lb/ft²**		
No.	Cell Type	Anneal	Cell* Size	Cell* Thick.	Cover Thicknes	BOL η (%)	SW Loss	Cell* Cost ($/W)	Spec. P. (W/kg)	P. Densit (W/m2)	Areal D. (lbs/ft2)	Spec. P. (W/kg)	P. Densit (W/m2)	Areal D. (lbs/ft2)	Spec. P. (W/kg)	P. Densit (W/m2)	Areal D. (lbs/ft2)	Spec. P. (W/kg)	P. Densit (W/m2)	Areal D. (lbs/ft2)
1	α-Si	N	12x13 in.	2μ	40 mils	10.0	0.85	2.50	19.0	90.1	0.972	21.8	88.2	0.828	27.8	81.7	0.602	n/a	n/a	n/a
2	α-Si	N	12x6.5 in.	2μ	8 mils	10.0	0.85	8.50	35.3	97.2	0.565	45.4	95.2	0.429	77.7	88.2	0.233	n/a	n/a	n/a
3	α-Si	N	12x13 in.	2μ	2μ	10.0	0.85	15.00	3.9	8.8	0.465	5.4	8.7	0.331	11.6	8.0	0.142	28.4	8.8	0.063
4	α-Si	N	12x13 in.	2μ	1 mil	10.0	0.85	20.00	42.7	99.2	0.476	58.2	97.2	0.342	121.2	90.0	0.152	266.5	97.2	0.075
5	Si BSR	N	2.5x5.0 cm	8.0 mils	2 mils	12.2	1.00	247.00	33.3	89.6	0.551	42.3	88.3	0.428	59.7	81.0	0.278	n/a	n/a	n/a
6	Si BSFR	N	2.5x5.0 cm	8.0 mils	2 mils	14.6	1.00	269.00	32.3	87.0	0.551	41.1	85.8	0.428	57.6	78.2	0.278	n/a	n/a	n/a
7	Si BSFR	N	2.5x5.0 cm	2.7 mils	2 mils	13.5	1.00	526.00	37.7	92.7	0.503	49.3	91.3	0.379	73.3	81.9	0.229	n/a	n/a	n/a
8	GaAs	N	4.0x4.4 cm	5.5 mils	3 mils	18.2	1.00	1350.00	45.0	131.2	0.597	56.3	127.4	0.463	77.0	117.7	0.313	n/a	n/a	n/a
9	GaAs	N	4.0x4.4 cm	8.0 mils	4 mils	18.2	1.00	909.00	41.2	134.0	0.666	50.4	127.9	0.520	65.9	119.1	0.370	n/a	n/a	n/a
10	α-Si	Y	12x13 in.	2μ	40 mils	10.0	0.95	2.50	20.3	96.5	0.972	23.4	94.5	0.828	29.8	87.5	0.602	n/a	n/a	n/a
11	α-Si	Y	12x6.5 in.	2μ	8 mils	10.0	0.95	8.50	37.8	104.2	0.565	48.7	102.0	0.429	83.2	94.5	0.233	n/a	n/a	n/a
12	α-Si	Y	12x13 in.	2μ	2μ	10.0	0.95	15.00	46.9	106.3	0.465	64.4	104.1	0.331	139.5	96.4	0.142	340.9	105.2	0.063
13	α-Si	Y	12x13 in.	2μ	1 mil	10.0	0.95	20.00	45.7	106.3	0.476	62.3	104.1	0.342	129.8	96.4	0.152	288.3	105.2	0.075

* = cell OR module ** = Areal Density + Peripheral Density

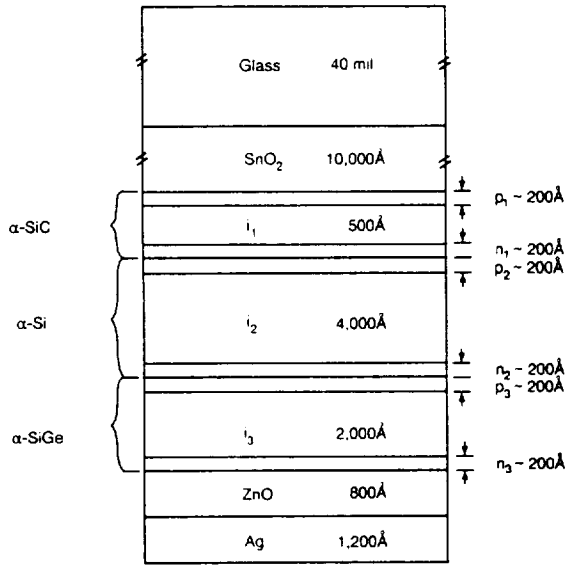

Figure 1: Cross Section of Triple Junction Solar Cell

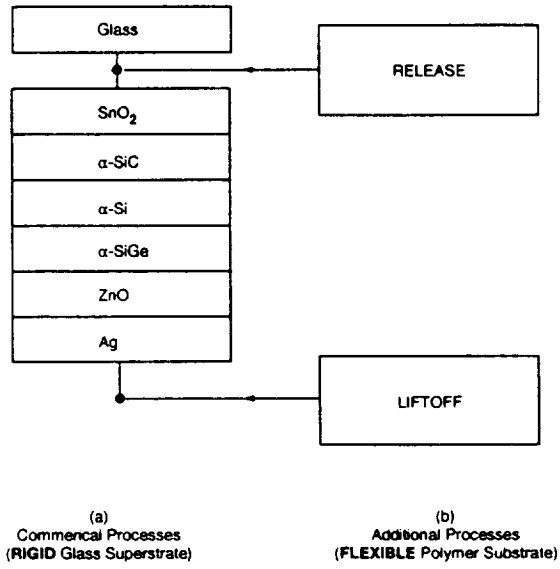

Figure 2: Total α-Si Processes

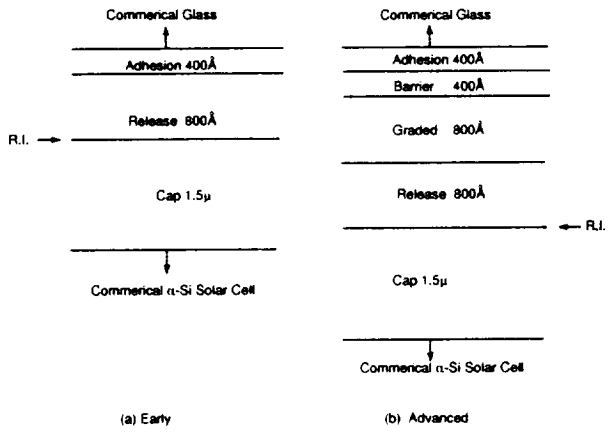

Figure 3: Release Process (a) Early (b) Advanced

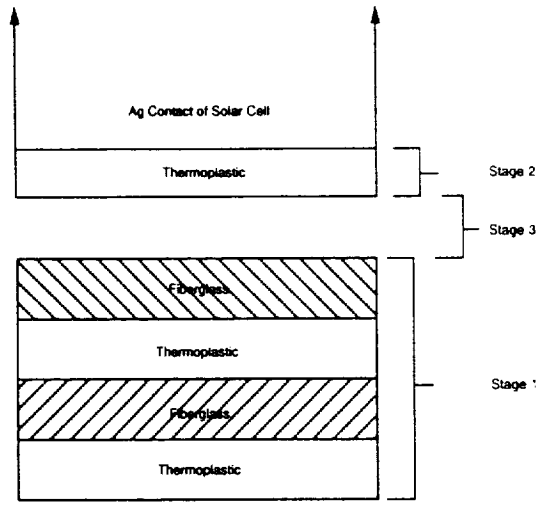

Figure 4: Liftoff Process

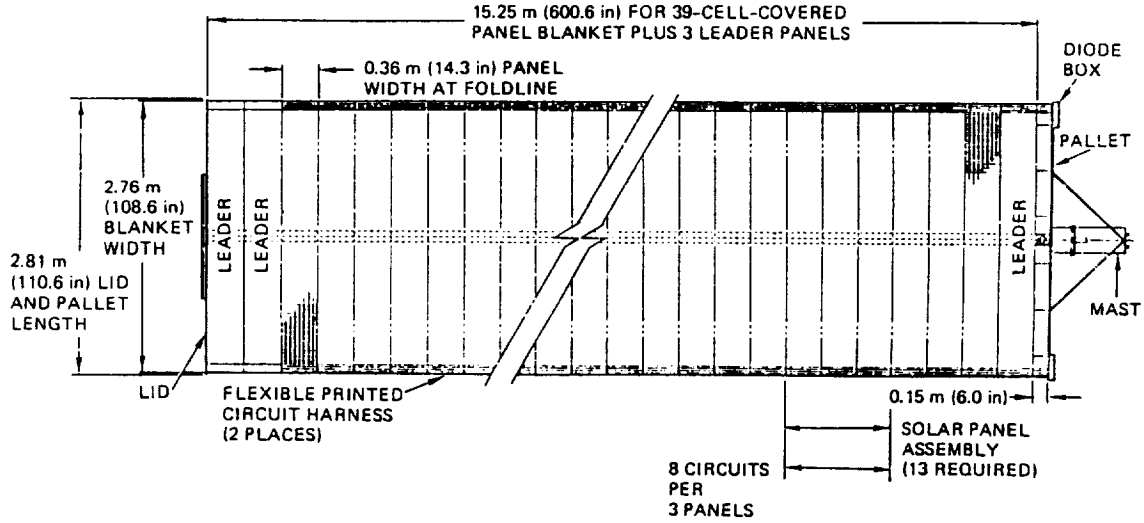

Figure 5: Full Scale APSA Structure

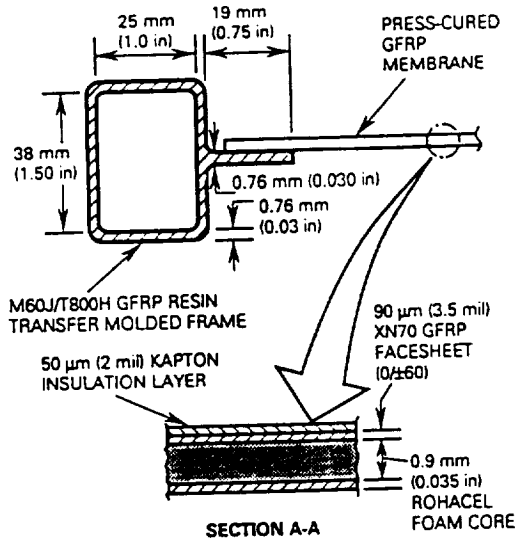

Figure 6: Framed Membrane Structure

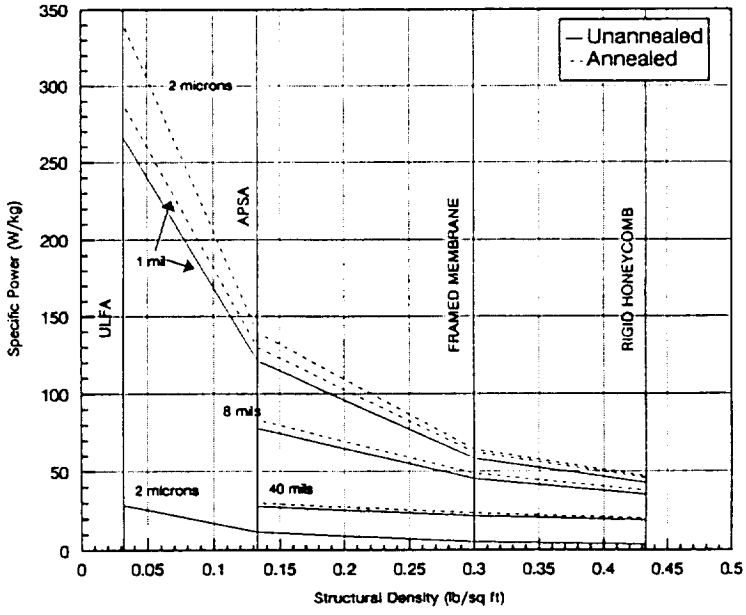

Figure 7: Comparison - α-Si vs. Structure

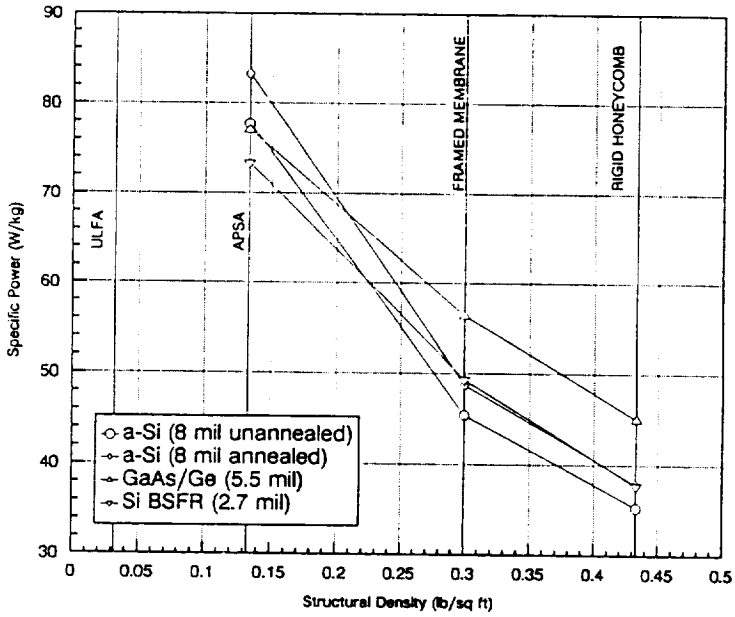

Figure 8: Comparison - Conservative α-Si with Best Crystalline vs. Structure

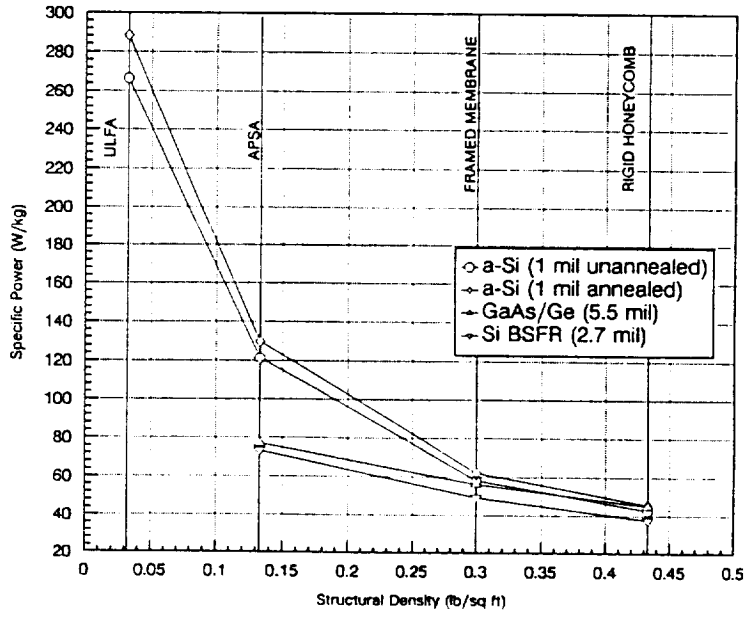

Figure 9: Comparison - Best Cases vs. Structure